Solar Phys (2010) 267: 203–216
DOI 10.1007/s11207-010-9645-x

Latitudinal and Solar-Cycle Variations of the White-Light Corona from SOHO/LASCO Observations

V.G. Fainshtein · D.M. Tsivileva · L.K. Kashapova

Received: 14 January 2010 / Accepted: 21 September 2010 / Published online: 21 October 2010

Abstract SOHO/LASCO data were used to obtain the latitudinal and radial distributions of the brightness of the K- and F-corona in the period of 1996 – 2007, and their solar-cycle variations were studied. Then an inversion method was employed to obtain the radial distributions of the electron density $N_e(R, \theta)$ for various latitude values on the coronal images. Our values of $N_e(R, \theta)$ are in good agreement with the findings of other authors. We found that in an edge-on streamer belt the electron density, like the K-corona brightness, varies with distance more slowly in the near-equatorial rays than in near-polar regions. We have developed a method for assessing the maximum values of the electron density at the center of the face-on streamer belt in its bright rays and depressions between them. Not all bright rays observed in the face-on streamer belt are found to be associated with an increased electron density in them. Mechanisms for forming such rays have been suggested.

Keywords Electron density · K- and F-corona · White-light corona

1. Introduction

The total surface brightness B of the white-light corona is the sum of the brightness of the K- and F-corona (B_K and B_F): $B = B_K + B_F$. The K-corona is formed by photospheric light scattered by free electrons in the coronal plasma, while the F-corona is formed by light scattered by dust particles in the solar system. To find the physical parameters of the coronal plasma and properties of the coronal dust component, we have to isolate B_K and B_F separately from the total brightness of the white-light corona. Several methods have been proposed for working out this problem. In 1950 – 1960, the Grotrian (1934) method was employed to separate the brightness of the K- and F-corona (Blackwell and Petford, 1966). It worked on the principle of measuring the ratio of the depths of Fraunhofer lines in the spectra of the photosphere and of the white-light corona.

V.G. Fainshtein (✉) · D.M. Tsivileva · L.K. Kashapova
Institute of Solar-Terrestrial Physics RAS SB, P.O. Box 291, 664033 Irkutsk, Russia
e-mail: vfain@iszf.irk.ru

The brightnesses of the K- and F-corona are often separated by the method relying on the measurements of the total brightness and total polarization degree of the white-light corona as well as on the calculations of the polarization degree of the K-corona assuming spherical symmetry (van de Hulst, 1950; Koutchmy, 1994; Lamy *et al.*, 1997). The F-corona is supposed to be non-polarized. This means that this method is applicable only for $R \leq 5R_{\odot}$, because the F-corona is polarized above $R \approx 5R_{\odot}$ (Koutchmy and Lamy, 1985; Mann, 1992). Here R is the radius in the plane of the sky drawn from the solar disk center to an observation point, and $R_{\odot}$ is the solar radius.

Another method for calculating the brightness of the K- and F-corona (Saito, Poland, and Munro, 1977) makes use of the distributions of the radial electron density (N_{e}) previously found from measurements of the polarized brightness $pB(R)$. They are substituted into the integral relation which relates $B_{\mathrm{K}}(R)$ to N_{e}, under the assumption that the electron density solely depends on the radius from the Sun's center.

In 2001, Hayes, Vourlidas, and Howard (2001) proposed a new method for separating the brightnesses of the K- and F-corona using SOHO/LASCO data. It does not rely on such simplifying assumptions as the absence of polarization of the F-corona over all distances and the spherical symmetry of the K-corona.

For several decades, the electron density in the corona was derived from the measurements of the polarized brightness by means of the inversion method put forward by van de Hulst (1950). Hayes, Vourlidas, and Howard (2001) developed the inversion method to determine the electron density from the brightness of the K-corona. These methods are imperfect because they rely on the assumption that the coronal plasma is spherically symmetric. This is known to be a rough approximation for the real corona. The coronal plasma is inhomogeneous at all scales and locations. Thernisien and Howard (2006) have proposed a method using a "newly developed forward modeling technique" for finding the three-dimensional distribution of the electron density. This method does not assume spherical symmetry of the corona, and their results indicated that the electron density varies as much as ten times in various streamer-belt areas.

In this study, we employ the Hayes – Vourlidas – Howard (HVH) method to obtain the brightness distributions of the K- and F-corona as a function of latitude, in the radius range of $R = (2.5 - 30)R_{\odot}$ in the years 1996 – 2007, covering a whole solar cycle. The brightness values of the K-corona at different areas and in different orientations (about the plane of the sky) of the streamer belt are used to obtain the radial electron-density distributions in the streamer belt and at various nearby latitudes.

2. Data and Methods of Analysis

In the present analysis, we employ the images of the corona of the processing level L1, calibrated in terms of the solar brightness, from SOHO/LASCO C2 and C3 data for 1996 – 2007 (http://sharpp.nrl.navy.mil/cgi-bin/swdbi/lasco/images/form). We use the HVH method to separate the brightnesses of the K- and F-corona. In this method, the brightness of the F-corona in each pixel in an image of the white-light corona is found as the minimum brightness value for the time interval of 56 days multiplied by a correction factor $K \leq 1$ depending on the distance to the solar disk center. This time interval is centered at the date for which B_{K} and B_{F} are separated. In this method, we assume that the brightness of the F-corona does not change within the period under study. We also assume that K is independent of latitude and time.

We employ the HVH inversion method to find the electron density N_{e} in the corona. This method gives the radial distribution of the electron density from the calculated values of

the brightness of the K-corona $B_K(R)$. Besides, we propose and test a method of finding the line-of-sight maximum electron density, max $N_e^{SB}(R,\theta)$, for a part of the streamer belt viewed face-on. This method is described in detail in Section 4.

The configuration of the coronal streamer belt is determined based on the shape of the magnetic neutral line on the source surface (*i.e.*, on a sphere with radius $R_s = 2.5R_\odot$) obtained from the potential-field approximation of the coronal magnetic field at WSO (http://quake.stanford.edu/~wso/coronal.html).

3. Radial and Latitudinal Variations of the Brightness of the F-corona during the Solar Cycle

Figures 1 and 2 present examples of latitude distributions of the brightness of the K- and F-corona. Figure 1 shows a streamer-belt area extended in latitude (θ) on the east limb near

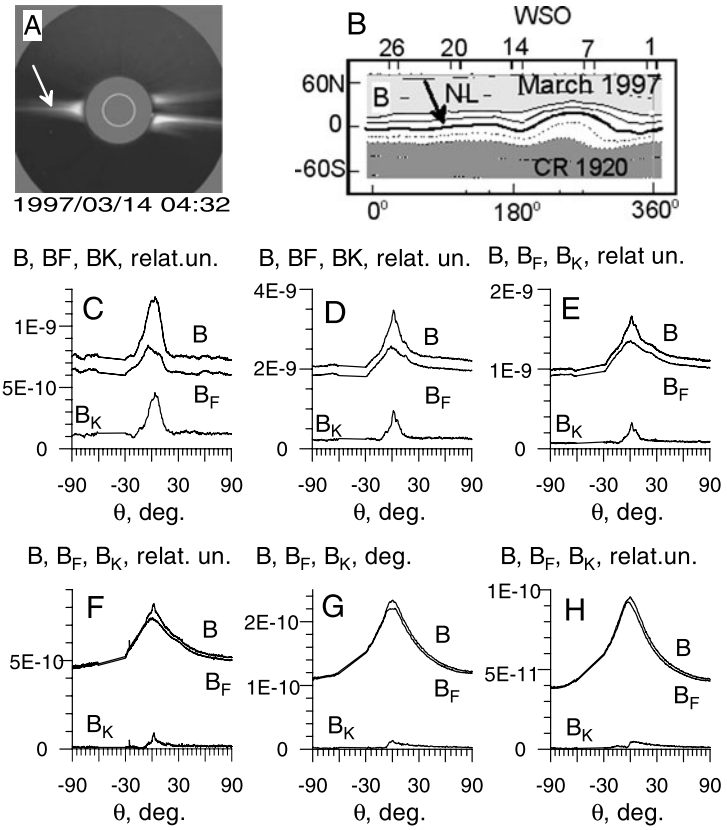

Figure 1 (A) The white-light corona on 14 March 1997. (B) The neutral line (NL) on the source surface is derived from calculations of the magnetic field in the corona in the potential-field approximation (http://quake.stanford.edu/~wso/coronal.html). (C – H) The latitude distributions of the total brightness of the white-light corona $B(\theta)$, and the brightness of the F- and K-corona ($B_F(\theta)$, and the brightness $B_K(\theta)$) for 14 March 1997 (15.35 UT for C2, 15.44 UT for C3) at $R = 2.5$, 3.5, 4.5, 6, 10, and 15 $R_\odot$ (the east limb). Over the area $-60° \lesssim \theta \lesssim -30°$ where the distributions of $B(\theta)$, $B_F(\theta)$ and $B_K(\theta)$ on the east limb are affected by the coronagraph's structural element, the values are replaced by the line segments which join the values of B, B_F, B_K at $\theta \approx -30°$ and $\theta \approx -60°$.

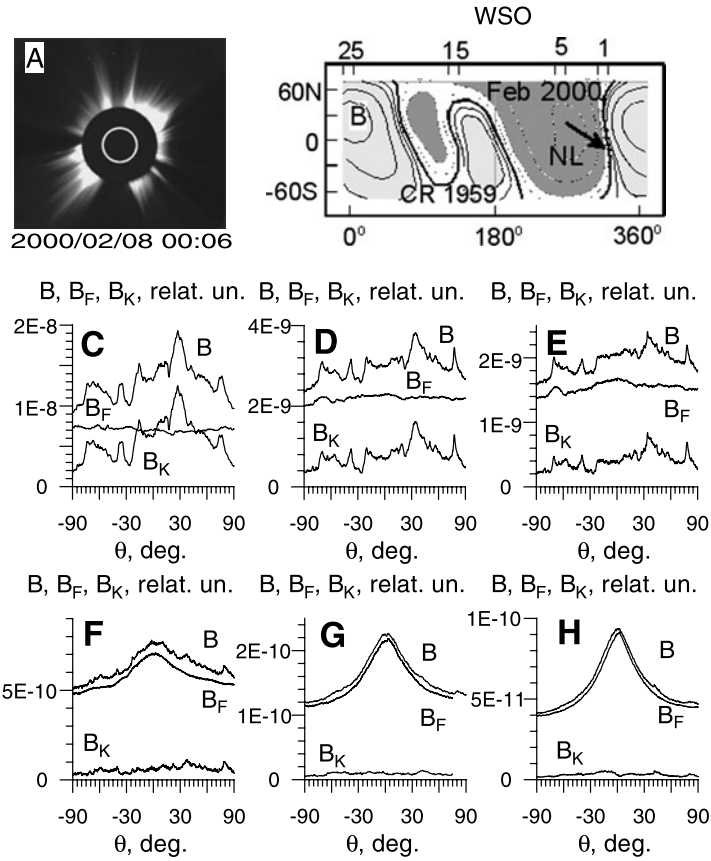

Figure 2 The same as Figure 1, but for 8 February 2000 (00.06 UT for C2 and 00.18 UT for C3), on the west limb.

the equator and almost perpendicular to the plane of the sky – the streamer belt viewed edge-on (14 March 1997). This is evidenced by the shape of a segment of the magnetic neutral line on the source surface near the central meridian on 20 – 22 March 1997 (Figure 1B). This results in a bright ray that appears in the coronal image near the equator on the east limb (Figure 1A). To this ray corresponds the brightness peak of the K-corona near the equator (Figures 1C – 1H).

Figure 2 shows similar data as Figure 1, but for the solar activity maximum of 8 February 2000, when the streamer-belt area, extended in latitude (several tens of degrees) and almost perpendicular to the equator (see Figure 2B), was in the vicinity of the plane of the sky on the west limb (the belt of streamers viewed face-on). In this case, a large number of bright rays can be observed over a wide range of latitudes in the plane of the sky on the west limb. These rays manifest themselves in the brightness distributions of the K-corona $B_{\mathrm{K}}(R,\theta)$ (Figures 2C – 2H).

We have studied the properties of parameters characterizing the radial brightness distributions of the F-corona over the solar cycle: the maximum value in latitude (max B_{F}), the values at the poles (B_{FS}, B_{FN}), and ratios $\frac{\max B_{\mathrm{F}}}{B_{\mathrm{FS}}}$ and $\frac{\max B_{\mathrm{F}}}{B_{\mathrm{FN}}}$, *etc.* (Figure 3). Figures 3A – 3D imply the following.

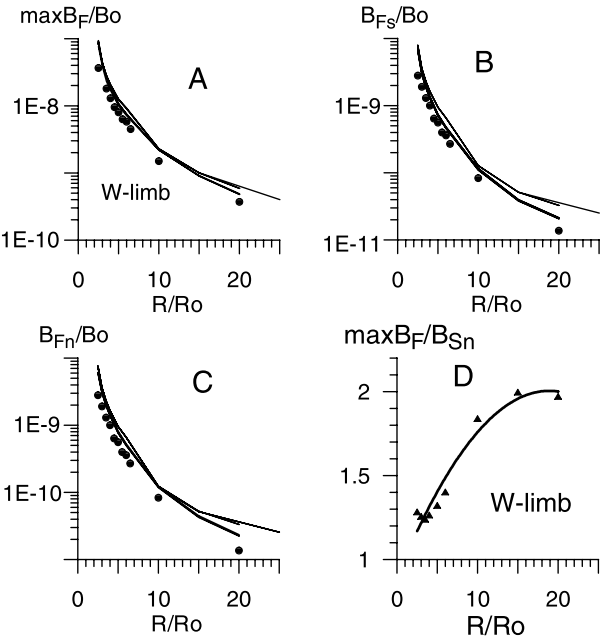

Figure 3 Radial distributions over the years 1997 – 2007 of (A) the maximum brightness of the F-corona (max B_F), the brightness of the F-corona at (B) the north (B_{FN}) and (C) south (B_{FS}) poles, and (D) the time-averaged $\frac{\max B_F}{B_{FN}}$ ratio. The filled circles are the values of $B_F(R)$ at the equator and the pole from Koutchmy and Lamy (1985).

i) max B_F, B_{FS} and B_{FN} decrease monotonically with distance R.

ii) In the events under study, max B_F varies with distance R on the average more slowly than B_{FN} (B_{FN}) does.

iii) The F-corona becomes more and more homogeneous in latitude as we look closer to the Sun's surface.

The results similar to our *i*) – *iii*) have been obtained in Saito, Poland, and Munro (1977) and in Koutchmy and Lamy (1985). However, they compared the radial brightness distributions of the F-corona at the pole and the equator, whereas we took the maximum brightness of the F-corona within $\pm 6^\circ$ about the equator (and even $>6^\circ$ in some cases) to compare it with B_{FN} and B_{FS}.

Figures 3A – 3C imply that max $B_F(R)$, $B_{FS}(R)$ and $B_{FN}(R)$ vary with time. We assume that the revealed variations in these parameters are not associated with their dependence on the phase of solar cycle, but occur due to: *i*) inaccuracy in the separation of the K- and F-corona, and/or *ii*) inclination of the plane of the ecliptic with respect to the solar equator. The latter causes the line of sight to cross the F-corona at various angles within a year. The annual brightness variations of the F-corona may also be produced by variations in the Sun – Earth distance. The absence of the dependence of the latitude distribution of the brightness of the F-corona on the phase of solar cycle at large distances ($R = (20-25)R_\odot$) has been shown in Fainshtein (2007). It has also been demonstrated by him that within a year the brightness distribution of the F-corona observed at $R = (20-25)R_\odot$ varies considerably, in much the same way as in Figures 3A – 3C. Note that the effect of the inclination of the ecliptic to the solar equator also shows up in the north – south asymmetry in terms of $B_F(\theta)$. For example, we found $B_F(90^\circ) > B_F(-90^\circ)$ in the cases considered.

4. The Brightness of the K-corona and the Electron Density as a Function of Latitude at Various Distances

4.1. The Brightness of the K-corona

Our analysis of the brightness of the K-corona $B_K(R,\theta)$ and the electron density $N_e(R,\theta)$ is limited by the LASCO C2 field of view. Nevertheless, it provides a maximum accuracy in separating the K- and F-corona and finding $N_e(R,\theta)$ from $B_K(R,\theta)$ values. Figures 4A and 4B present examples of the brightness distributions of the K-corona in latitude at various distances R for two periods of solar activity: 14 March 1997 and 8 February 2000.

Note the typical asymmetry in the latitude distributions of the K-corona brightness northward and southward of the equator for the first event. It shows up in the difference between $B_K(R)$ values near the poles over all distances, mainly due to the ecliptic being inclined relative to the solar equator. Moreover, at $R > 4R_\odot$ one can observe a relative increase in the brightness of the K-corona with distance over the range of $10^\circ \lesssim \theta \lesssim 45^\circ$ compared to the latitude range $45^\circ \lesssim \theta \lesssim 90^\circ$. It is still unknown whether this feature is a real property of the corona or is due to inaccuracy in separating the K- and F-corona.

The second event is peculiar because the brightness of the K-corona varied at a different rate with distance R, both in various higher-brightness rays and in brightness depressions between the rays. As a result the relative brightness in different streamer-belt elements varied with distance.

Figure 5A presents $B_K(R,\theta)$ at various latitudes for the 14 March 1997 image of the corona.

The figure implies that the brightness of the K-corona decreases with distance faster in coronal regions outside the streamer belt ($\theta = \pm 30^\circ; \pm 60^\circ; \pm 90^\circ$) than within the streamer belt (at the latitude $\theta = 0$ and in the brightness maximum in the near-equatorial rays). This agrees with the results obtained by Koutchmy and Lamy (1985) for the equator and the poles.

For comparison this figure also presents the $B_K(R)$ distribution for the edge-on streamer-belt area at the end of January 2004, taken from Thernisien and Howard (2006). It is evident that their $B_K(R)$ distributions closely match max $B_K(R)$ in the edge-on streamer belt of 14 March 1997.

Figure 5B presents the brightness distributions of the K-corona $B_K(R)$ in several bright rays and brightness depressions between them on 8 February 2000 (west limb). In Figure 4B, these rays and brightness depressions are marked by numerals on the $B_K(R = 3.5R_\odot, \theta)$ distribution. This figure implies that the rate of decrease of $B_K(R)$ with distance differs both in different rays and in different depressions (compare, for example, rays "3" and "9", depressions "d3" and "d4").

For comparison, Figure 5(B) shows the max $B_K(R)$ distribution on 14 March 1997 (east limb). One may notice the fact that the brightness in some rays is twice as large as the maximum K-corona brightness in the streamer belt of 14 March 1997. A probable cause of this will be discussed below.

4.2. The Electron Density

The radial brightness distributions of the K-corona of $B_K(R,\theta)$ found at different latitudes θ were used to obtain the radial distributions of the electron density $N_e(R,\theta)$ in the edge-on streamer belt and its vicinity for 14 March 1997 (Figure 6A). The distributions of $N_e(R,\theta)$

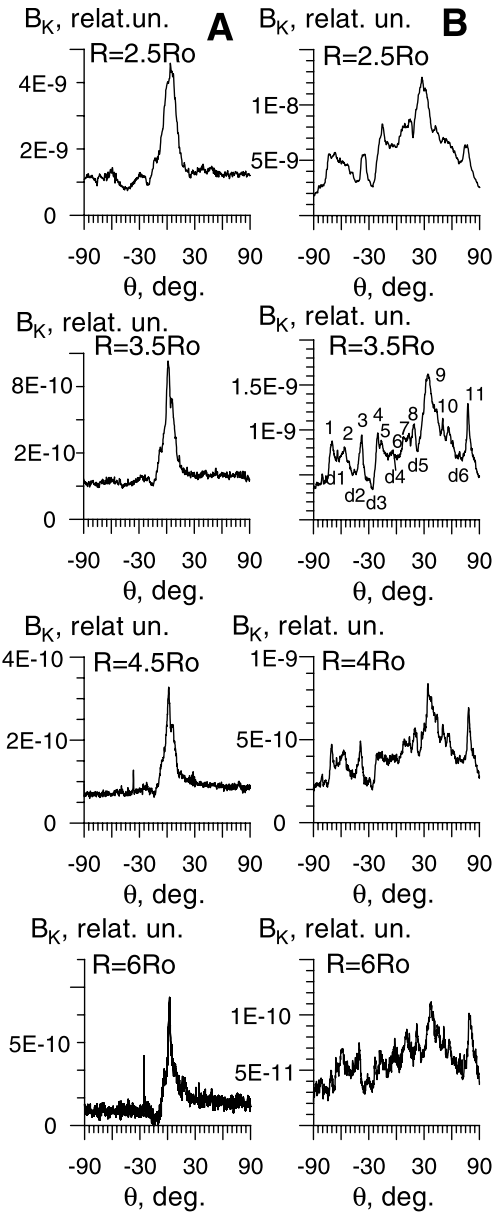

Figure 4 The brightness distributions of the K-corona in latitude θ at different distances R: (A) 14 March 1997 corona (east limb) and (B) 8 February 2000 corona (west limb). Some bright rays and brightness depressions are marked by symbols 1, 2 (rays), and d1, d2 (brightness depressions) in panel (B), $R = 3.5R_{\odot}$.

were also calculated in higher-brightness rays and depressions between the rays for 8 February 2000 in the face-on streamer belt (Figure 6B). As was mentioned above, we applied the HVH inversion method to estimate the electron density in the corona.

For comparison, Figure 6A also shows the boundaries of the variations of the electron density in the streamer belt taken from Thernisien and Howard (2006) and radial distributions of the electron density at the equator and the pole for the 26 February 1998 corona from Hayes, Vourlidas, and Howard (2001) and data obtained by other researchers (Saito, Poland, and Munro, 1977).

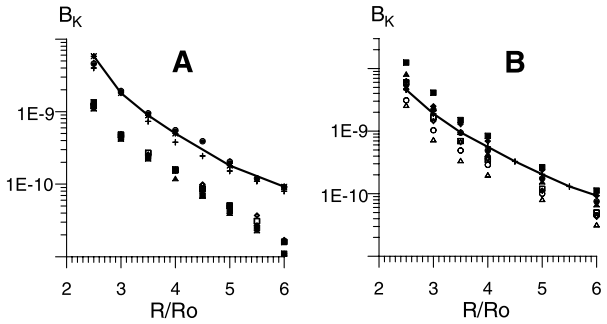

Figure 5 Radial brightness distributions of the K-corona at various latitudes $B_K(R,\theta)$. (A) 14 March 1997 (east limb). The dots indicate the brightness maximum, and filled triangles, filled squares, and filled diamonds correspond to $\theta=-90°$, $\theta=-60°$, $\theta=-30°$. Similar open symbols correspond to $\theta=90°$, $\theta=60°$, and $\theta=30°$. The crosses are for $\theta=0°$. The solid line with an asterisk shows the distribution of the brightness corresponding to the edge-on streamer belt in January 2004, taken from Thernisien and Howard (2006). (B) 8 February 2000 (west limb). The filled symbols and asterisks indicate rays 4 – 8, and the open symbols indicate brightness depressions d3 – d5. The solid line with crosses shows the brightness distribution for the streamer belt viewed edge-on on 14 March 1997 (east limb).

The electron densities at latitudes outside the streamer belt ($\theta=\pm30°, \pm60°, \pm90°$) are found to be lower than the electron density within the belt. A typical thickness of this streamer belt is about 12.5°. Figures 4(A) and 6(A) imply that the electron density depends only slightly on latitude out of the streamer belt, especially in the southern part of the corona.

We also used the inversion method to find the electron density in different streamer-belt areas viewed face-on (Figure 6B). This figure implies that the electron densities in most rays and depressions in question almost uniformly fill the range of $N_e(R)$ variation in the streamer belt calculated by Thernisien and Howard (2006). The exception is the brightest ray, "9", at $R=(2.5-4)R_\odot$ and the depression "d2" at $R=(4-6)R_\odot$. At $R=(2.5-3)R_\odot$, the electron density in "9" is about 1.5 times as large as the upper boundary of $N_e(R)$ found by Thernisien and Howard (2006) for the streamer belt in January 2004. We suppose that the edge-on streamer belt, like the face-on one, consists of a sequence of rays with high plasma density and depressions between the rays with low density. Indirect evidence for this is a great number of higher-brightness rays observed in the visual analysis of the coronal images of 1996 – 1997 (http://lasco-www.nrl.navy.mil/daily_mpg/) when the parts of the streamer belt were located at relatively small angles to the equator and were projected onto the plane of the sky.

Hence it is not the maximum N_e at each R ($\max N_e(R,\theta)$) that is found by the inversion method for the edge-on streamer belt, but a certain value resulting from the variations of the electron density in the streamer belt that are averaged in longitude. This value may be substantially smaller than $\max N_e(R)$ in regions with high electron density. Our estimations for the edge-on streamer belt testify that $\max N_e(R) \geq 2N_e^i(R)$, where $N_e^i(R)$ is the electron density obtained by the inversion method. Applying this relation to the face-on streamer-belt area yields $\max N_e(R)_{ray9} \geq 3N_e^{HB}(R)$, where $N_e(R)_{ray9}$ is the electron density in ray "9", and N_e^{HB} is the electron density at the upper limit of the electron-density variation in Thernisien and Howard (2006). This difference is too large to result only from the N_e variation with time in the corona, from February 2000 to January 2004. We assume that the brightness enhancement in ray "9" is mainly not due to the increase of the electron density, but to another effect, of adjacent, nearly horizontal area (*i.e.*, located along the line

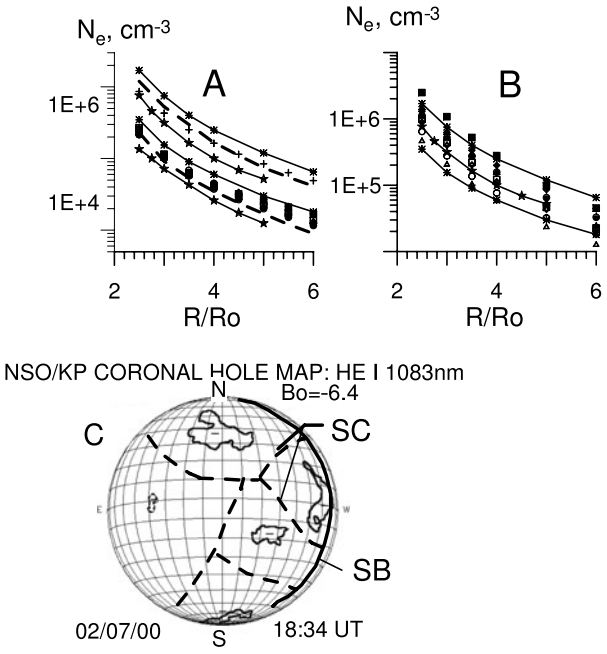

Figure 6 (A) The radial distributions of the electron density $N_e(R)$ obtained by the inversion method in the 14 March 1997 corona (east limb). The symbols which indicate different latitudes are the same as in Figure 5. Dashed lines show the $N_e(R)$ distributions at the equator (the top curve) and the poles (the bottom curve) for 26 February 1998 (east limb) taken from Hayes, Vourlidas, and Howard (2001). The solid line with filled asterisks mark the $N_e(R)$ distributions at the equator (the top curve) and the poles (the bottom curve) taken from Saito, Poland, and Munro (1977). (B) The electron density as a function of R in the face-on streamer belt of 8 February 2000 (west limb). The filled circles, triangles, squares and diamonds are for rays 3, 4, 6, 11; similar open symbols are for depressions d2, d3, d4, d6. For comparison, the solid lines with asterisks in both panels (A, B) demonstrate the boundaries of the variation of the electron density in the streamer belt calculated in Thernisien and Howard (2006). The asterisks mark the $N_e(R)$ distributions at the equator taken from Saito, Poland, and Munro (1977). (C) Approximate relative positions of the coronal streamer belt (solid line) and chains of coronal streamers (dashed lines) as well as coronal holes are superposed on the He I 10830 Å map.

of sight) of the coronal streamer chain (CSC) to the vertical streamer-belt area. Recall that CSCs divide coronal holes with equal magnetic-field polarity (Eselevich, Fainshtein, and Rudenko, 1999). They are also observed as streamers in the corona ("pseudostreamers", Wang *et al.*, 2007). CSC configurations can be computed using the "potential field – source surface" model (Eselevich, Fainshtein, and Rudenko, 1999). Regular calculations of these configurations on the source surface are performed on http://bdm.iszf.irk.ru/.

Illustrating possible CSC configurations on 8 February 2000, Figure 6C shows the boundaries of coronal holes (obtained in the 10830 Å image obtained at the Kitt Peak National Observatory on 7 February 2000), with their magnetic-field polarity indicated. It also depicts schematically the magnetic neutral line (an analogue of the streamer belt (SB)) and CSCs expected on the source surface. For convenience of analysis, the coronal holes, SBs, and CSCs are superposed onto the same surface in the figure. It can be seen that one CSC is adjacent to the neutral line at a latitude close to the latitude of ray "9", while the others have latitudes close to ray "3" and "4" .

Let us pay attention to yet another ray, "11". We think that the basic cause of the emergence of this ray is the bending of the streamer belt near the north pole rather than an

increase in the electron density in the belt (see the shape of the neutral line on the source surface, Figure 1B). Along the line of sight a part of the edge-on streamer belt is recorded as a higher-brightness area, as a result.

Hence, some higher-brightness rays observed in the face-on streamer belt are due to the edge-on streamer-belt area near the poles or to the streamer chain arranged almost horizontally to the streamer belt, but not to the increase of the electron density in these rays. The edge-on streamer-belt areas can also appear between circumpolar bending of the face-on streamer belt. The brightness in all such rays may vary with distance differently from the brightness in the rays whose brightness comes from an increase in their electron density. Among the rays in which brightness enhancement is associated with an increase of the electron density may be rays "4", "5", and other rays, un-numbered in Figure 4B.

We also attempted to determine the maximum electron densities (max N_e^{SB}) within the face-on streamer belt as a function of θ and R. For this purpose we applied the following technique. First, we determined the K-corona brightness $B_K^{SB}(R,\theta)$, which is only due to scattering of the photospheric radiation by streamer-belt electrons: $B_K^{SB}(R,\theta) = B_K(R,\theta) - B_K^B(R,\theta)$. Here $B_K(R,\theta)$ is the total K-corona brightness, and $B_K^B(R,\theta)$ is the background K-corona brightness out of the streamer belt. The latitude-dependent background brightness at a fixed radius was determined from the total K-corona brightness observed a few days before 8 February 2000. In that case, the streamer-belt contribution to the total K-corona brightness may be ignored. According to the calculations made by Hundhausen (1993), a bright feature, with an angular size of 10° and rotated by 65° longitude from the limb, makes a relative contribution of about 3% to the total K-corona brightness. In our case, an analogue of such a bright feature was a vertical streamer-belt area. A convenient date for estimating the background brightness, in our case, was 3 February 2000, when the vertical part of the streamer belt was inclined by 66° to the plane of the sky. This implies that the streamer-belt contribution to the total K-corona brightness may be neglected. On that day there were no other vertical parts of the streamer belt near the plane of the sky. No coronal mass ejections, which could distort the background, were recorded in the latitude range $-40° < \theta < 40°$ on 3 February 2000.

Figure 7A shows the distributions $B_K(R = 3.5R_\odot, \theta)$ on 3 February 2000 and $B_K(R = 3.5R_\odot, \theta)$ on 8 February 2000 as an example. This figure demonstrates the correspondence between higher-brightness rays as well as depressions recorded on 8 February 2000 and their related features on $B_K(R = 3.5R_\odot, \theta)$ on 3 February 2000. The displacement of these features toward the poles on 3 February 2000 as compared to 8 February 2000 is associated with the fact that the apparent latitudes of the streamer-belt features were displaced in longitude about the plane of the sky and exceeded the true latitudes of these features (Hundhausen, 1993).

Figure 7B presents radial distributions of $B_K^{SB}(R,\theta) = B_K(R = 3.5R_\odot, \theta,$ 8 February 2000$) - B_K(R = 3.5R_\odot, \theta,$ 3 February 2000$) = B_K(R,\theta) - B_K^B(R,\theta)$ for two rays and two depressions within $(-40° < \theta < 40°)$. The choice of this latitude interval for the analysis is due to yet another reason. In the southern near-polar area of 3 February 2000, the contribution from the edge-on streamer-belt area to the K-corona brightness increased because the area appeared closer to the plane of the sky.

To determine the maximum electron densities in individual rays and depressions, let us make use of the following well-known fact. At $R \geq 3R_\odot$ the thickness of the streamer belt is small and is from 7° to 15° in the heliographic coordinate system, according to our estimates. This conclusion can be drawn from the observations of the edge-on streamer belt (Figure 4A). By using the relation $\max B_K^{SB}(R)\Delta_{SB} = \int B_K^{SB}(R,\theta)\,d\theta$, we found the values of Δ_{SB} for several streamer-belt areas viewed edge-on and situated near the equator in 1996 – 1997. The average value for these areas $\langle\Delta_{SB}\rangle$ is approximately 11.5° (0.2 rad).

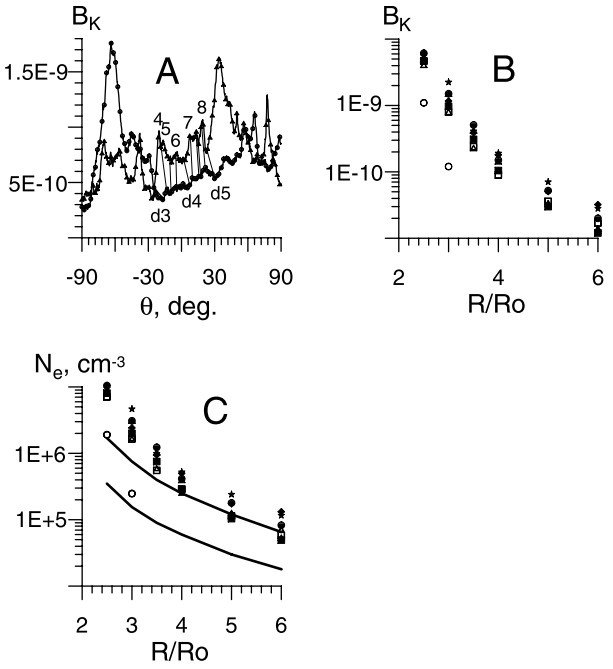

Figure 7 (A) The latitude distribution of the K-corona brightness at $R = 3.5R_{\odot}$, when the face-on streamer-belt area is in the plane of the sky (top curve, 8 February 2000) and when this area is displaced by $\approx 66^{\circ}$ from the plane of the sky (bottom curve, 3 February 2000). The line segments show the correspondence between the same streamer-belt structures for two $B_{\mathrm{K}}(R,\theta)$ distributions. (B) The radial distributions of the K-corona brightness expected from scattering of photospheric radiation by streamer-belt electrons alone ($B_{\mathrm{K}}^{\mathrm{SB}}(R,\theta)$) for rays 4 – 8 and depressions d3 – d5. (C) The radial distributions of maximum electron densities in the streamer belt obtained in a thin streamer-belt approximation. The filled circles, triangles, squares, diamonds, and asterisks are for rays 4 – 8, and open symbols are for depressions d3 – d5. The solid lines mark the boundaries of the variation of the electron density in the streamer belt calculated by Thernisien and Howard (2006).

The maximum electron density max $N_{\mathrm{e}}(R)$ along the line of sight in higher-brightness rays or depressions between them for a "thin" streamer belt can be derived from the following relation:

$$\max N_{\mathrm{e}}(R,\theta) = \frac{1.38\times 10^{14} B_{\mathrm{K}}^{\mathrm{SB}}(R,\theta)(R/R_{\odot})\sin\alpha}{\langle \Delta_{\mathrm{SB}} \rangle}\ [\mathrm{cm}^{-3}] \tag{1}$$

where α is the inclination angle of the streamer belt with respect to the plane of the ecliptic. Here $\alpha \approx 80^{\circ}$. Equation (1) was derived from the equation relating $N_{\mathrm{e}}(R)$ to $B_{\mathrm{K}}(R)$ in the "point" Sun approximation presented in Hundhausen (1993). When deriving Equation (1), we assumed that the parameter describing the degree of limb darkening was 0.5.

Figure 7C demonstrates the radial distributions of electron density in the streamer belt derived from Equation (1) for two rays whose brightness increase is due to the increase of the electron density and for two depressions. It is obvious that in all the rays and depressions under study the calculated maximum electron density exceeds the upper boundary of the range of $N_{\mathrm{e}}(R)$ found by Thernisien and Howard (2006) in the streamer belt.

It is still uncertain whether the result is correct or not. Equation (1) has two parameters that were calculated approximately, namely $B_{\mathrm{K}}^{\mathrm{SB}}(R,\theta)$ and Δ_{SB}. Our analysis has revealed that the streamer-belt thickness, Δ_{SB}, varies roughly between 7° and 15°. This means that the resulting max $N_{\mathrm{e}}(R)$ values cannot be explained by the error in determining this parameter only. If the result is erroneous, the origin of the overestimated max $N_{\mathrm{e}}(R)$ values should be the error in determining $B_{\mathrm{K}}^{\mathrm{SB}}(R,\theta)$. The K-corona brightness of the background plasma might have increased from 3 to 8 February 2000, involving a decrease in $B_{\mathrm{K}}^{\mathrm{SB}}$ and thus in max $N_{\mathrm{e}}(R)$.

5. Conclusion

The main research results may be stated as follows.

i) We have obtained the brightness distributions of the K- and F-corona as a function of latitude and distance R to the solar disk center for 1997 – 2007, using LASCO C2 and C3 data and the HVH method.

ii) We have found that in all phases of solar activity: (1) the maximum brightness of the F-corona max $B_{\mathrm{F}}(R)$ as well as $B_{\mathrm{FS}}(R)$ and $B_{\mathrm{FN}}(R)$ decrease monotonically with distance R; (2) the F-corona brightness decreases more rapidly with distance R at the pole than near the equator; (3) the F-corona is more homogeneous in latitude closer to the solar surface.

These conclusions agree with the known results obtained by Saito, Poland, and Munro (1977) and by Koutchmy and Lamy (1985).

iii) The analysis of the brightness distributions of the K-corona derived from LASCO C2 images taken at the onset of solar activity increase (14 March 1997), and at the solar maximum (8 February 2000) has revealed that: *a*) the K-corona brightness outside the edge-on streamer belt ($\theta > 15°$) decays more rapidly than in the coronal streamer belt of 14 March 1997; *b*) the K-corona brightness varied with distance at different rates in different rays and depressions between them in the face-on streamer belt of 8 February 2000.

iv) The inversion method was employed to obtain the radial distributions of the electron density $N_{\mathrm{e}}(R,\theta)$ for various latitude values on the coronal images of 14 March 1997 and 8 February 2000. In both cases, the values of $N_{\mathrm{e}}(R,\theta)$ we found in the streamer-belt area are in agreement with the findings of Thernisien and Howard (2006) as well as with the radial distributions of the electron density at the equator obtained by other authors. The distributions of $N_{\mathrm{e}}(R,\theta)$ in the streamer belt derived from the coronal image of 14 March 1997 compare well with those obtained by other researchers for polar regions. We found that in the edge-on streamer belt the electron density, like the K-corona brightness, varies with distance more slowly in the near-equatorial rays than in near-polar regions. Not all bright rays observed in the face-on streamer belt are found to be associated with an increased electron density in them. Mechanisms for forming such rays have been suggested.

v) We have developed a method for assessing the maximum values of the electron density (max $N_{\mathrm{e}}(R,\theta)$) at the center of the face-on streamer belt (8 February 2000) in its bright rays and depressions between them. The maximum electron densities we obtained using this method in various streamer-belt structures turned out to be 2 – 3 times higher than those found by Thernisien and Howard (2006) in the streamer belt. It is still unclear whether the relatively large max $N_{\mathrm{e}}(R,\theta)$ values we obtained in the face-on streamer belt are true values of the electron density in the streamer belt or are due to the inaccuracy in determining max $N_{\mathrm{e}}(R,\theta)$.

Let us make some comments on the methods we used in this work and the results obtained.

The first question we must address is the accuracy of the HVH method for separating the brightnesses of the K- and F-corona. The method assumes implicitly that the radiation registered by the coronagraph includes only the photospheric light scattered by free electrons in the coronal plasma and by cosmic dust particles. Actually, despite the fact that to separate the brightness of the K- and the brightness of the F-corona we have used the calibrated data of the processing level L1 in which the parasitic stray light contribution is minimized, it is impossible to rule out completely the contribution of this or another type of spurious radiation. Nevertheless, the HVH method allows the K-corona brightness to be separated relatively accurately by varying the coefficient K, a parameter in this method (see Section 2). As a criterion of the accuracy in determining the K-corona brightness we can make use of the proximity between the radial electron-density distributions obtained by the inversion method using the K-corona brightness and polarization brightness. In this case, when applying the HVH method the residual spurious radiation contributing to the observed coronal images will be added to the F-corona brightness and vice versa. Therefore, we can achieve a relatively accurate separation of the F-corona brightness by varying the coefficient K and using the brightness values of the F-corona obtained by other methods as a criterion. In this case, however, the error in finding the K-corona brightness increases because of spurious radiation.

Recall that it is necessary to make an absolute brightness calibration of the image of the white-light corona to derive the electron density. The accuracy in finding the electron density in the coronal plasma depends largely on the accuracy of such a calibration. This work relies on already calibrated coronal images of processing level L1 obtained from the LASCO C2 and C3 data or by means of special analysis programs in SolarSoft developed by the LASCO team. The calibration of the LASCO C3 coronagraph is described in detail in Morrill *et al.* (2006). It is worthy of note that it is one of the most effective methods for calibrating the coronal emission to have been developed and applied to analyze the coronal images obtained during eclipses. The method is based on the comparison between the brightness of the white-light corona and the radiant flux from very well calibrated stars (Koutchmy *et al.*, 1978). Observing stars is the unique and fundamental method of in-flight photometric calibration adopted in the LASCO coronagraphs.

One more remark is about the influence of time variations of the corona on the determination of the electron density N_e by the inversion method. As the inversion method is applied to an individual image, the accuracy of the calculated N_e may be affected by possible changes in the coronal plasma during the exposure of the image. It takes minutes for the LASCO coronagraphs to take an image, but there will be no significant changes in the coronal plasma density during this period. It means that in fact these changes of the coronal plasma will only slightly influence the accuracy in N_e. A more significant source of the inaccuracy in determining N_e in the corona may be the error in determining the K-corona brightness which results from the two-month change in the F-corona brightness. Recall that it takes 56 days to determine the minimum brightness of the corona and the F-corona in each observation pixel by the HVH method. Due to the inclination of the plane of the ecliptic to the solar equator, and for other possible reasons (see Section 2), the F-corona brightness varies with time during this period. According to Fainshtein (2007), a change in the F-corona brightness may amount to several per cent at large distances during this period. This means that at a certain moment the K-corona brightness found by the HVH method may differ from the true value. However, there is reason to believe that this difference is small: radial brightness distributions of the K-corona we

found and the electron densities found by the inversion method agree with results obtained by other authors.

Let us make a remark about the nature of bright coronal rays we analyzed in this paper. We have come to the conclusion that there are three mechanisms for forming such rays:

i) Projection of the edge-on streamer-belt area on the plane of the sky.
ii) Overlapping of a part of the coronal streamer chain which is nearly parallel to the solar equator and the face-on streamer belt.
iii) Increase of the electron density in areas with small angular sizes in the face-on streamer belt.

However, it is entirely possible that there are other mechanisms for forming bright rays in the corona as well. It is known that during an eclipse one can observe bright linear or curved sheets which can extend up to distances of several solar radii. The nature of many of these sheets is not understood yet. Some sheets are likely to be continuations of bright rays observed in the field of view of LASCO C2 and resulting from the projection of streamer belt areas (chains) on the plane of the sky, in the lower corona. They may also appear when various sporadic flows (coronal mass ejections, jets, shock waves, *etc.*) propagate in the corona. Then again, they may be isolated streamers or current sheets appearing in regions of large magnetic-field gradients and having higher plasma density. Extending in the field of LASCO C2 (C3), such sheets may give rise to some of the observable bright rays.

Acknowledgements The authors appreciate and thank the anonymous referee for his/her constructive comments and suggestions. SOHO is a project of the ESA and NASA international cooperation. This work was supported by the Government Grant "Leading Scientific Schools of the Russian Federation" N NSH 4741.2006.2 and by the Program for Fundamental Research of RAS Presidium N 16. We express our gratitude to M.V. Eselevich for development of the program for calculating the electron density in the corona by means of the inversion method.

References

Blackwell, D.E., Petford, A.D.: 1966, *Mon. Not. R. Astron. Soc.* **131**, 383.
Eselevich, V.G., Fainshtein, V.G., Rudenko, G.V.: 1999, *Solar Phys.* **188**, 277.
Fainshtein, V.G.: 2007, *Astron. J.* **84**, 1135 (in Russian).
Grotrian, W.: 1934, *Z. Astrophys.* **8**, 124.
Hayes, A.P., Vourlidas, A., Howard, R.A.: 2001, *Astrophys. J.* **548**, 1081.
Hundhausen, A.J.: 1993, *J. Geophys. Res.* **98**, 13,191.
Koutchmy, S.: 1994, *Adv. Space Res.* **14**(4), 29.
Koutchmy, S., Lamy, P.L.: 1985, In: Giese, R.H., Lamy, P. (eds.) *Properties and Interections of Interplanetary Dust*, *IAU Colloq.* **85**, 63.
Koutchmy, S., Lamy, P., Stellmacher, G., DzuDzubenko, N.I., Ivanchuk, V.I., Popov, O.S., Rubo, G.A., Vsekhsvyatsky, S.K.: 1978, *Astron. Astrophys.* **69**, 35.
Lamy, P., Quemerais, E., Llebaria, A., Bout, R.A., Howard, R., Schwenn, R., Simnett, G.: 1997, In: Wilson, A. (ed.) *Proc. 5th SOHO Workshop, The Corona and Solar Wind near Minimum Activity*, *ESA SP-404*, 491.
Mann, I.: 1992, *Astron. Astrophys.* **261**, 329.
Morrill, J.S., Korendyke, C.M., Brueckner, G.E., Giovane, F., Howard, R.A., Koomen, M., *et al.*: 2006, *Solar Phys.* **233**, 331.
Saito, K., Poland, A.I., Munro, R.H.: 1977, *Solar Phys.* **55**, 121.
Thernisien, A.F., Howard, R.A.: 2006, *Astrophys. J.* **642**, 523.
van de Hulst, H.C.: 1950, *Bull. Astron. Inst. Neth.* **XI**(410), 135.
Wang, Y.-M., Biersteker, J.B., Sheeley, N.R. Jr., Koutchmy, S., Mouette, J., Druskmuller, M.: 2007, *Astrophys. J.* **660**, 882.